

Supporting Information

Ag-In-Zn-S quantum dots dominated interface kinetics in Ag-In-Zn-S/NiFe LDH composite towards efficient photo-assisted electrocatalytic water splitting

Dongxu Zhang^{1§}, Weixuan Dong^{1§}, Yanhong Liu^{1§}, Xiaoqing Gu³, Tianyu Yang³, Qiang Hong³, Di Li¹, Dongqi Zhang¹, Hongbo Zhou¹, Hui Huang³, Baodong Mao^{1,*}, Zhenhui Kang^{2,3*} and Weidong Shi^{1,*}

¹School of Chemistry and Chemical Engineering, Jiangsu University, 301 Xuefu Road, Zhenjiang 212013, China

²Macao Institute of Materials Science and Engineering, Macau University of Science and Technology, Taipa 999078, Macau SAR, China

³Institute of Functional Nano and Soft Materials (FUNSOM), Jiangsu Key Laboratory for Carbon-based Functional Materials and Devices, Soochow University, 199 Ren'ai Road, Suzhou 215123, China

**Corresponding authors E-mail: maobd@ujs.edu.cn (B.M.); zhkang@suda.edu.cn (Z.K.); swd1978@ujs.edu.cn (W.S.)*

Contents:

Total number of pages: 16

Total number of Figures: 14

Total number of Tables: 1

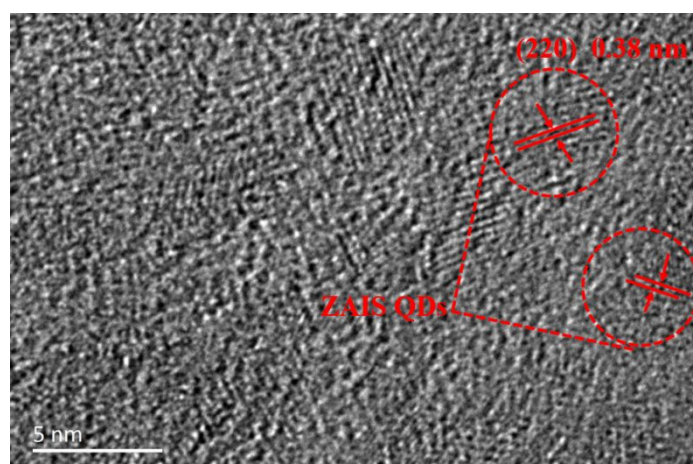


Figure S1. HRTEM image of the ZAIS QDs.

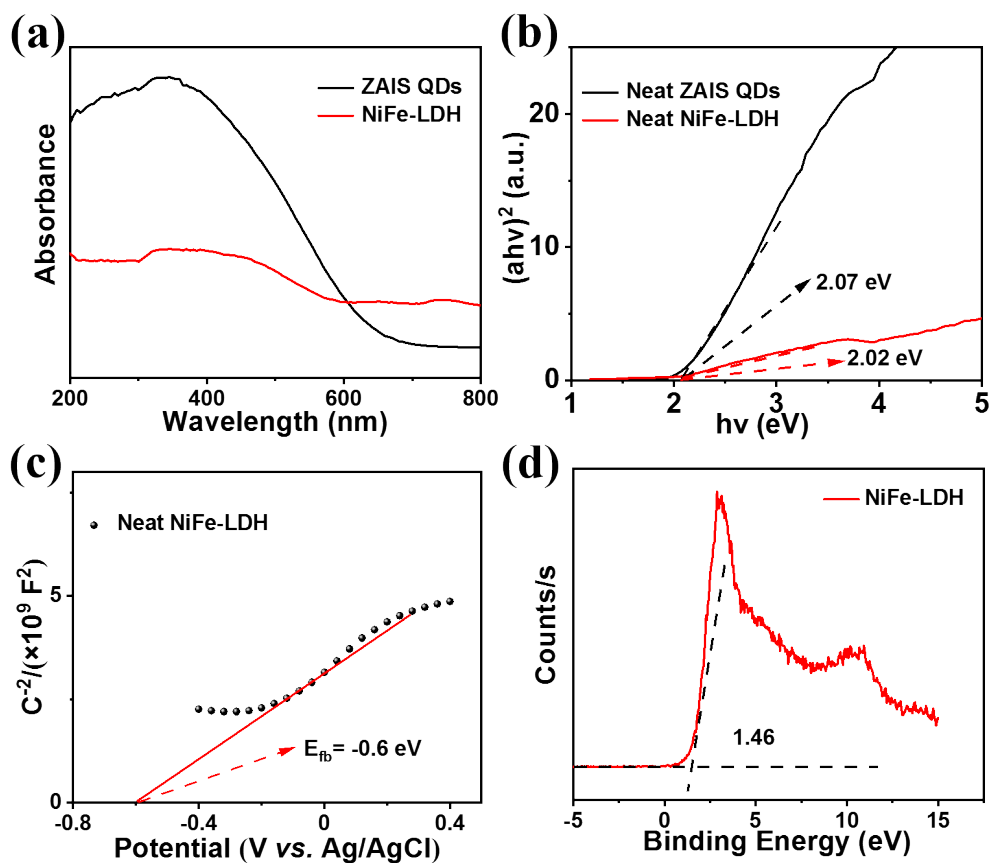


Figure S2. (a) UV-vis diffuse reflectance spectra for ZAIS QDs and NiFe LDH, (b) corresponding Tauc plot of $(\alpha h\nu)^2$ vs $h\nu$ for bandgap estimation. (c) Mott-Schottky (M-S) plots for NiFe LDH and (d) XPS valence band spectrum for NiFe LDH.

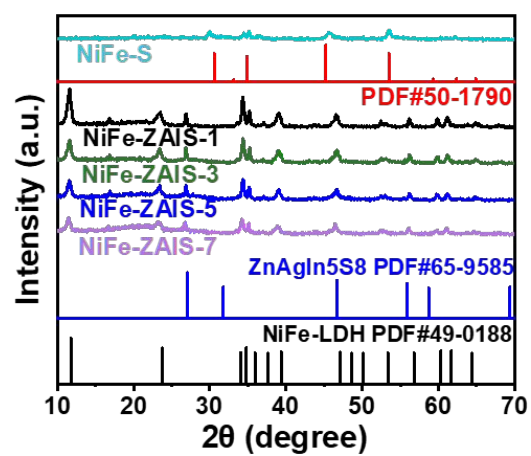


Figure S3. XRD patterns of NiFe-S, NiFe-ZAIS-1, NiFe-ZAIS-3, NiFe-ZAIS-5 and NiFe-ZAIS-7.

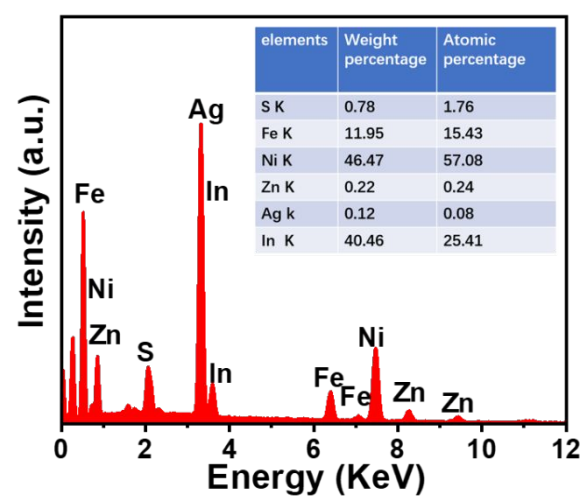


Figure S4. EDX of NF@NiFe-ZAIS-5.

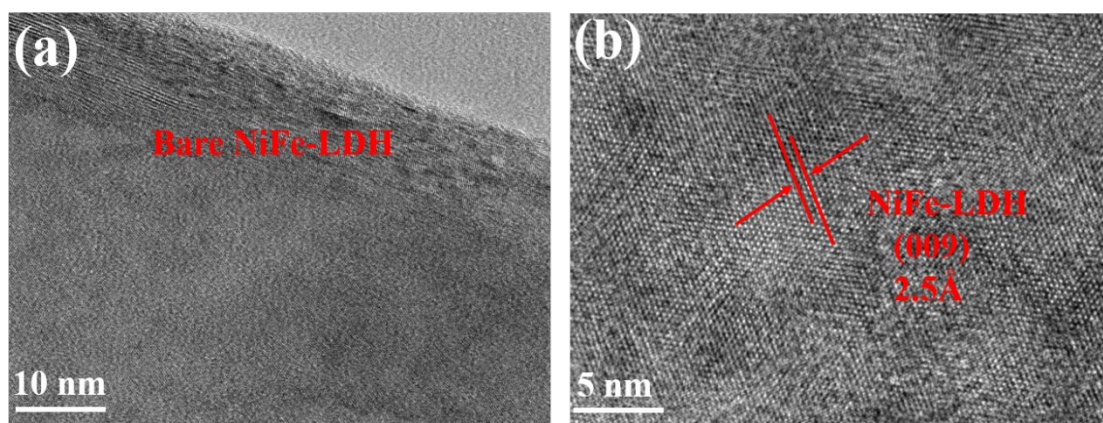


Figure S5. TEM (a) and HRTEM (b) images of NiFe LDH nanosheets.

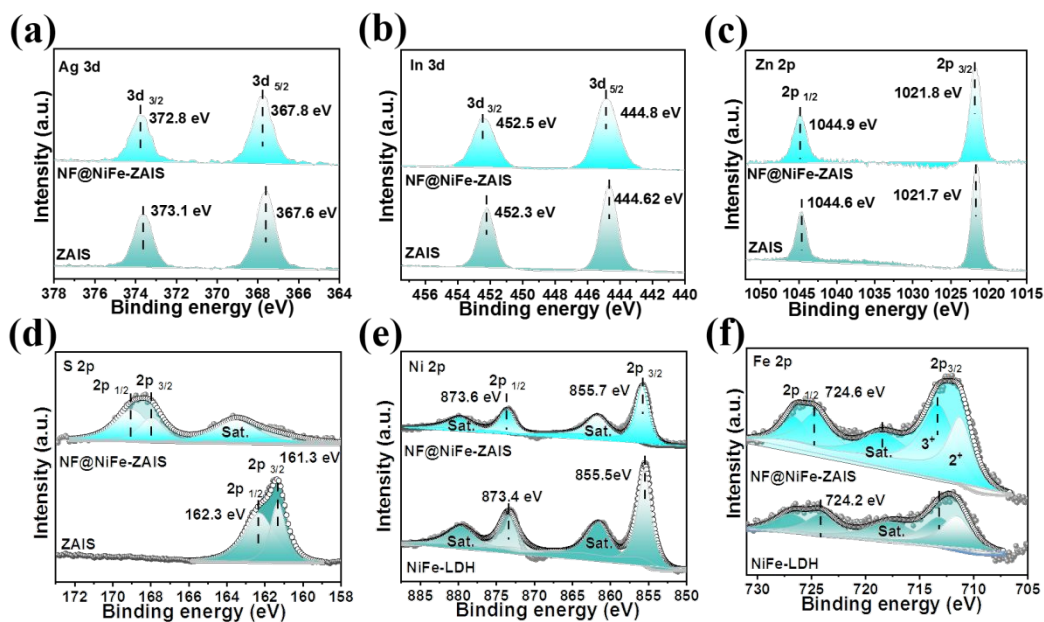


Figure S6. High-resolution XPS spectra of (a) Ag 3d, (b) In 3d, (c) Zn 2p, and (d) S 2p of ZAIS QDs and NiFe-ZAIS. (e) Ni 2p and (f) Fe 2p XPS spectra of NiFe LDH and NiFe-ZAIS.

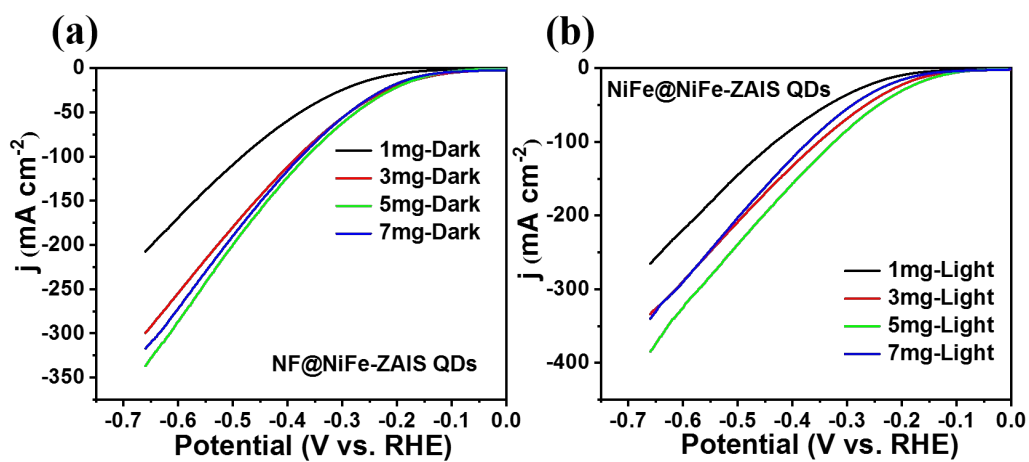


Figure S7. HER polarization curves of NF@NiFe-ZAIS with different amount of ZAIS QDs (1, 3, 5, and 7 mg) without (a) or with (b) illumination by Xe light under electrochemical test.

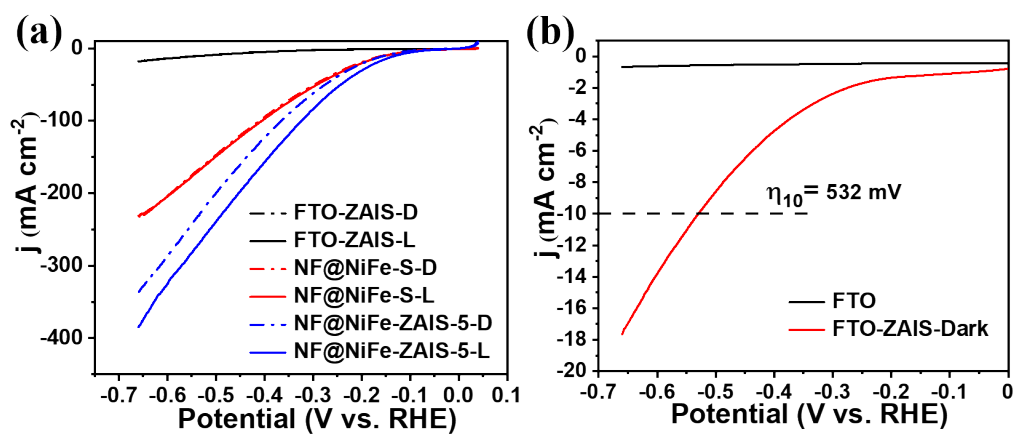


Figure S8. (a) HER polarization curves of FTO-ZAIS-D, FTO-ZAIS-L, NF@NiFe-S-D, NF@NiFe-S-L, NF@NiFe-ZAIS-5-D, and NF@NiFe-ZAIS-5-L in 1M KOH. (b) HER polarization curves of FTO and FTO-ZAIS-Dark in 1M KOH.

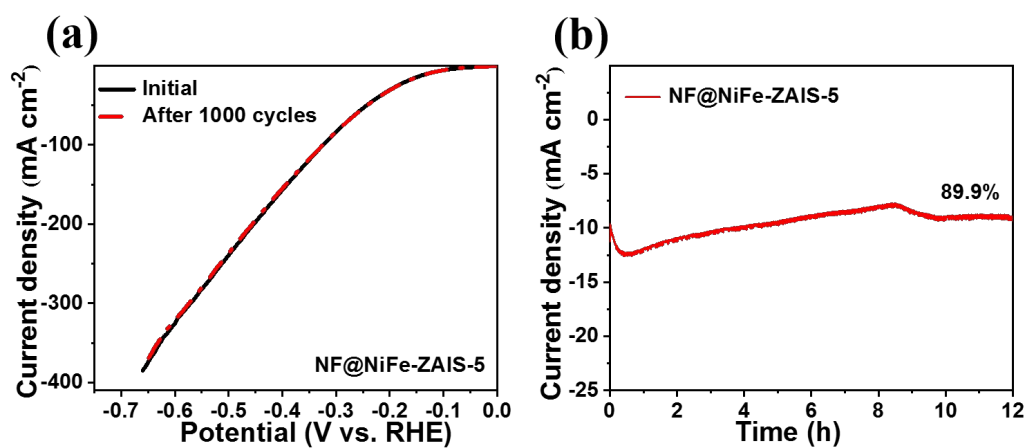


Figure S9. (a) Polarization curves of NF@NiFe-ZAIS-5 for the stability test after 1000 CV cycles.

(b) The long-term i-t curves of NF@NiFe-ZAIS-5 for the HER durability test at 10 mA cm⁻².

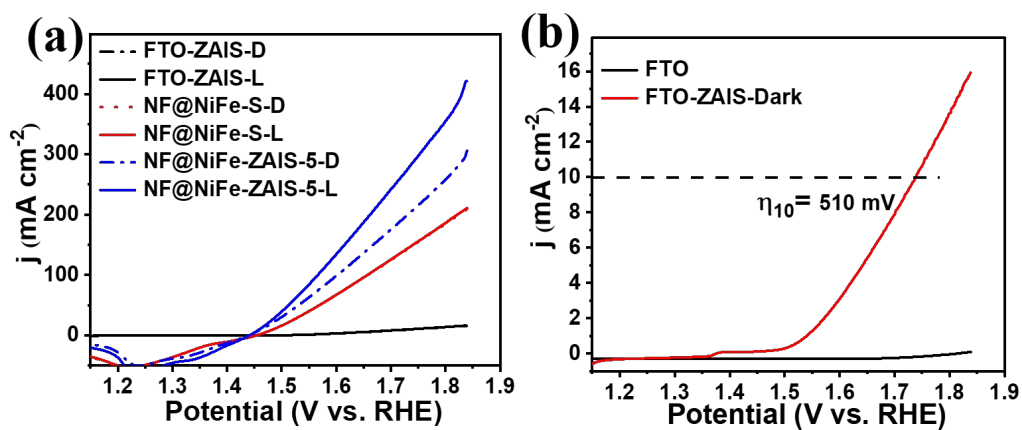


Figure S10. (a) OER polarization curves of FTO-ZAIS-D, FTO-ZAIS-L, NF@NiFe-S-D, NF@NiFe-S-L, NF@NiFe-ZAIS-5-D, and NF@NiFe-ZAIS-5-L in 1M KOH. (b) OER polarization curves of FTO and FTO-ZAIS-Dark in 1M KOH.

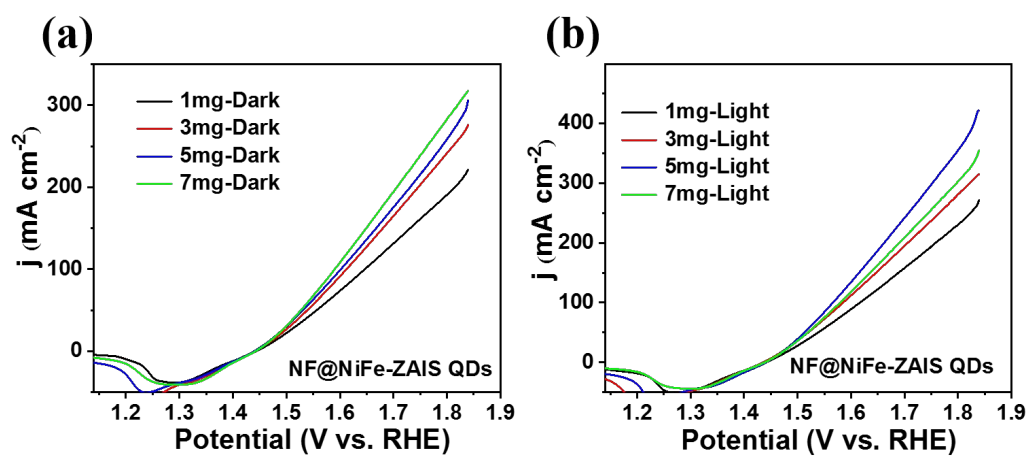


Figure S11. OER polarization curves of NF@NiFe-ZAIS with different amount of ZAIS QDs (1, 3, 5, and 7 mg) without (a) or with (b) illumination by Xe light under electrochemical test.

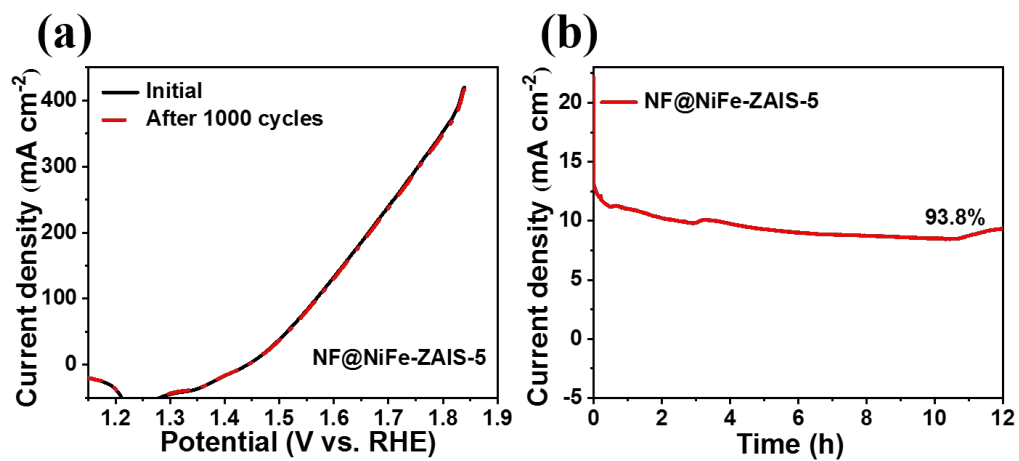


Figure S12. (a) Polarization curves of NF@NiFe-ZAIS-5 for the stability test after 1000 CV cycles. (b) The i-t curves of NF@NiFe-ZAIS-5 for OER durability test at 10 mA cm⁻².

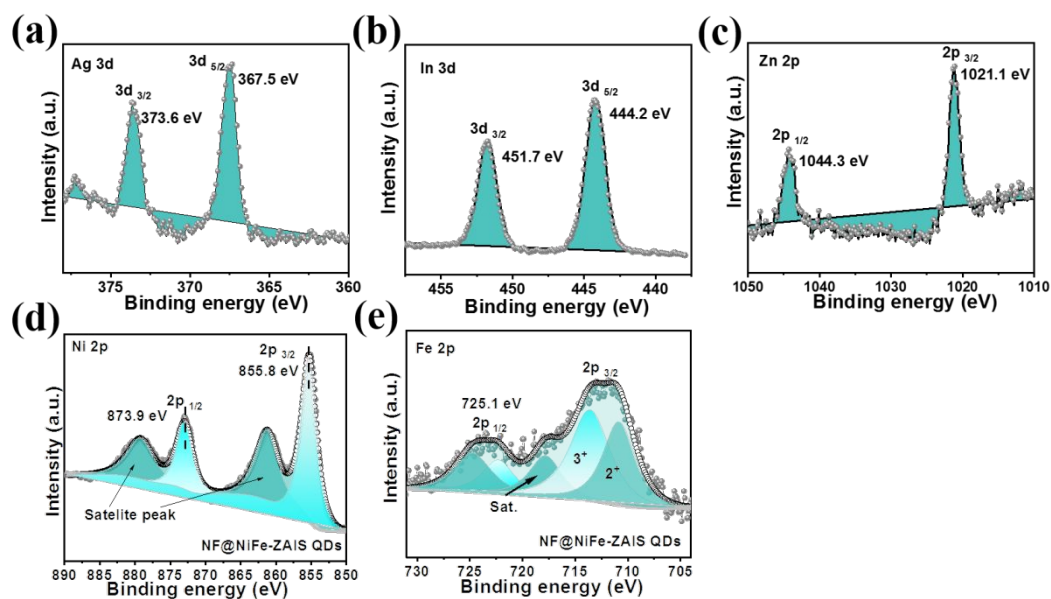


Figure S13. High-resolution XPS spectra of (a) Ag 3d, (b) In 3d, (c) Zn 2p, (d) Ni 2p and (e) Fe 2p for NF@NiFe-ZAIS QDs after P-EC stability test with light irradiation for 12 h.

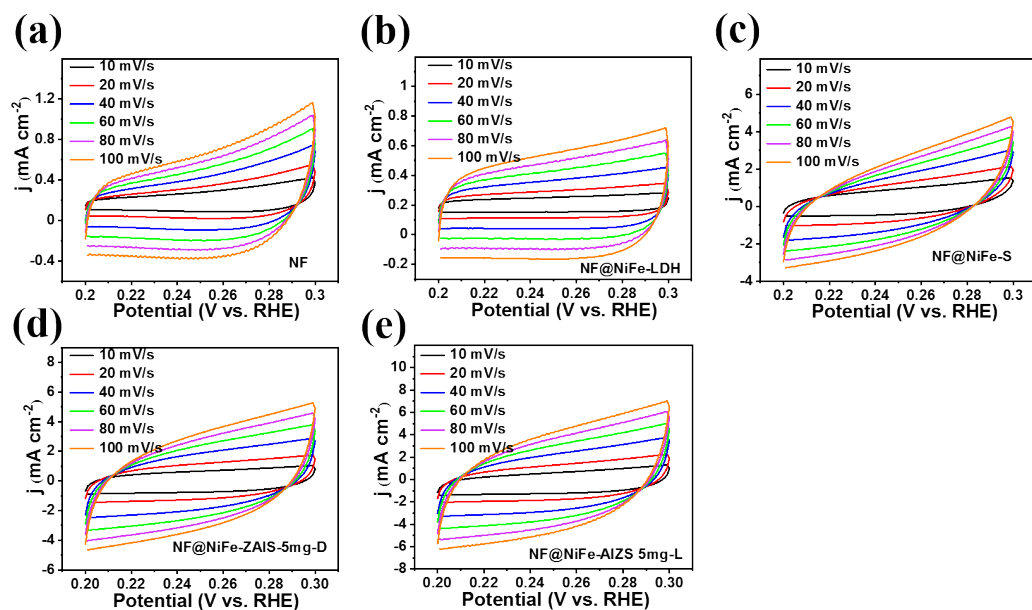


Figure S14. Cyclic voltammogram curves at different scan rates (from 10 mV/s to 100 mV/s) of (a) NF, (b) NF@NiFe-LDH, (c) NF@NiFe-S, (d) NF@NiFe-ZAIS-5mg-D, and (e) NF@NiFe-ZAIS-5mg-D.

Table S1. Corresponding fitting parameters of EIS data using the equivalent circuit in the inset in Figure 9d.

Samples	R_s (Ω cm ²)	R_{ct} (Ω cm ²)
NF	10.59	11.24
NF@NiFe-LDH	4.28	5.24
NF@NiFe-S	4.91	3.20
NF@NiFe-ZAIS-5-D	3.13	2.57
NF@NiFe-ZAIS-5-L	6.98	1.18